Available online at www.sciencedirect.com
SCIENCE DIRECT
Journal of Asian Earth Sciences 27 (2006) 358–370
Journal of Asian Earth Sciences
www.elsevier.com/locate/jaes

Characteristics of claystones across the terrestrial Permian-Triassic boundary: Evidence from the Chahe section, western Guizhou, South China

Suxin Zhang[a], Yuanqiao Peng[a,b,*], Jianxin Yu[a], Xinrong Lei[c], Yongqun Gao[d]

[a]Faculty of Earth Sciences, China University of Geosciences, Wuhan 430074, Hubei Province, People's Republic of China
[b]School of Ecology and Environment, Deakin University, Melbourne Campus, 221 Burwood Highway, Burwood VIC 3125, Australia
[c]Faculty of Material Science and Chemical Engineering, China University of Geosciences, Wuhan 430074, Hubei Province, People's Republic of China
[d]China University of Geosciences Press, Wuhan 430074, Hubei Province, People's Republic of China

Received 5 November 2004; revised 24 March 2005; accepted 19 April 2005

Abstract

X-ray diffraction (XRD), scanning electronic microscopy (SEM) and X-ray fluorescence spectroscopy (XFS) studies were undertaken for claystones and/or mudstones from the Chahe section—a terrestrial Permian-Triassic boundary (TPTB) section. Our results indicate that the compositions of claystones in the Permian-Triassic boundary (PTB) interval (Beds 66f–68) outlined by biostratigraphy are different from claystones and/or mudstones found either below or above the interval of the same section. The clay minerals in the claystones of the PTB interval are mainly composed of illite–montmorillonite interlayers, with a few montmorillonites and chlorites. The other claystones and/or mudstones underlying and overlying the PTB consist of chlorites and/or kaolinites. Some authigenic clastic minerals, such as hexagonal dipyramid quartz and zircons, are only found in claystones in the PTB interval from the Chahe section and some marine PTB sections in western Guizhou and eastern Yunnan, southwestern China. In addition, some elements are present in abnormal concentrations in the claystones of the PTB interval as well. Most important is that we found no spherules in all the claystones studied, indicating no evidence of an extraterrestrial impact during the Permian-Triassic transition. The particular characteristics of the TPTB claystones at the Chahe section indicate their volcanic origin and thus provide a reliable auxiliary event marker for high-resolution demarcation of the TPTB in South China. They are also indicative in the marine PTB claystones in South China. Thus, the PTB claystones can be used as auxiliary markers for high-resolution correlation of the PTB from marine facies to land in South China when direct fossil evidence in the PTB sequence is lacking.
© 2005 Elsevier Ltd. All rights reserved.

Keywords: Permian-Triassic boundary (PTB); Claystone; Chahe section; South China; X-ray diffraction (XRD); Scanning electronic microscopy (SEM); X-ray fluorescence spectroscopy (XFS)

1. Introduction

Claystones of special origin (for example, volcanism as proposed by Yin et al., 1992, and many others) are highly developed across the marine Permian-Triassic boundary (PTB) in South China. Such claystones are useful for investigation of processes and timing of the PTB mass extinction. Each clay bed across the PTB consists of interbedded illite and mixed illite–montmorillonite interlayers, with subordinate kaolinite occurring locally (Yang et al., 1993). Although the clay beds have been generally regarded to be of volcanic origin due to the presence of high temperature quartz, zeolite and relic tuffaceous textures within the clays (Yin et al., 1992), other scenarios are also possible. The scenario of an impact event associated with the Permian-Triassic transition remains controversial because reports on the Ir anomaly in the PTB claystones are usually inconsistent (see Yin et al., 1992 for review and references cited therein). However, some new evidences, including extraterrestrial fullerenes (Becker et al., 2001), meteoritic debris (Basu et al., 2003) and Fe–Ni–Si grains

* Corresponding author. Address: School of Ecology and Environment, Deakin University, Melbourne Campus, 221 Burwood Highway, Burwood VIC 3125, Australia.
E-mail address: ype@deakin.edu.au (Y. Peng).

1367-9120/$ - see front matter © 2005 Elsevier Ltd. All rights reserved.
doi:10.1016/j.jseaes.2005.04.007

(Kaiho et al., 2001) found in the PTB claystones, support an extraterrestrial origin, although there is still significant debate (Braun et al., 2001; Farley et al., 2001; Buseck, 2002; Koeberl et al., 2002; Erwin, 2003). On the other hand, Zhou et al. (1991) argued that the spherules found in the PTB claystones were of diverse origins, in that sanidine, picotitite and rutile spherules might be related to an impact event, and the apatite and organic spherules may be of biogenic origin, while the ferruginous spherules might be related to both. Whatever the origin of the PTB claystones, they are obviously isochronous and can be correlated regionally in South China (Yang et al., 1993; Peng et al., 2001) and as such are an excellent correlation marker for eventostratigraphy. Zircons are commonly found in the marine PTB claystones, and are useful for age determination of the PTB, although results are sometimes very different due to different testing methods (Renne et al., 1995; Bowring et al., 1998; Mundil et al., 2001, 2004).

Claystones were also found across the terrestrial Permian-Triassic boundary (TPTB) in western Guizhou and eastern Yunnan, southwestern China (Wang and Yin, 2001a,b). A study of the TPTB sections in western Guizhou and eastern Yunnan has revealed a stable set of claystone beds associated with the TPTB sections in the study area. Apart from their special origin by volcanism and/or extraterrestrial collision (Wang and Yin, 2001a,b), of particular interest is the regular vertical (stratigraphical) succession of the TPTB sequence, which is usually characterized by the vertical stacking of a clay and/or mudstone, followed by a muddy siltstone, which in turn is followed by a second clay and/or mudstone bed. This regular succession of claystone beds, which is common to all the marine PTB sections in South China, is similar to the PTB beds at the Meishan section, where it is characterized by two claystone beds (beds 25 and 26) in the lower part, a micrite bed (bed 27) in the middle, and another clay bed (bed 28) in the upper part. Elsewhere, Peng et al. (2001, 2002) have formally named this succession of PTB beds as the Permian-Triassic Boundary Stratigraphic Set (PTBST) in recognition of its stratigraphic persistence and stability across South China and therefore its potential as an alternative marker for recognizing and correlating PTB in both marine and non-marine PTB sections in South China. The concept has proved very useful for defining the PTB position in sections where no definitive biostratigraphic markers, such as the definite first appearance of conodont *Hindeodus parvus* (Kozur et Pjatakova), is available in South China (see Peng et al., 2001 for more details).

2. Geological setting and outline of stratigraphy

The Chahe section is located between the 31 and 32 km milestones of the country road from Heishitou Town to Haila Town, Weining City (Fig. 1). The section includes the upper half of the Upper Permian to lowermost Triassic Xuanwei Formation, the entire lowest Triassic Kayitou Formation (Wang, 2001, 2002) or Kayitou Bed (Nanjing Inst., 1980) and the lower part of the Lower to Middle Triassic Dongchuan Formation (Fig. 2).

2.1. Lithostratigraphy

The Xuanwei Formation is composed of terrestrial clastics (sandstones and siltstones), interbedded with coal beds and/or seams. The Xuanwei Formation is conformably overlain by the Kayitou Formation, which in lithology is almost the same as that of the Xuanwei Formation except that it lacks interbedded coal beds or seams. The Dongchuan Formation, conformably overlying the Kayitou Formation, is dominated by clastic sediments (sandstones and siltstones) of terrestrial origin as well.

There are clear differences in rock color between the Xuanwei, Kayitou and Dongchuan formations in the Chahe section. At the outcrop section, the grey to grey–green strata belong to the Xuanwei Formation, the variegated to the Kayitou Formation, and the purple to the Dongchuan Formation. The non-marine PTB strata in southwestern China all belong to these color types and can be well correlated lithologically and regionally (Peng et al., 2005).

2.2. Biostratigraphy

Only plant fossils and sporomorphs have been found in the Chahe section, western Guizhou (Wang and Yin, 2001a; Peng et al., 2005). Plant fossils are abundant mainly in the Xuanwei Formation, with very few species found in the Kayitou Formation and no intact plants found in the Dongchuan Formation (Fig. 2). Sporomorphs are also abundant in the Xuanwei Formation, but less so in the Kayitou Formation. Until now, no sporomorphs have been found in the Dongchuan Formation (Fig. 2). The PTB in the Chahe section marks the mass decrease of plants and the compositional change of plants from the dominance of Palaeozoic ferns and pteridosperms to the dominance of Mesozoic gymnosperms (Peng et al., 2005).

33 species of 19 genera of fossil plants have been discovered at the Chahe section, distributed in 19 beds from Bed 1 to Bed 69, all belonging to the upper part of the Xuanwei Formation (Nanjing Inst., 1980; Peng et al., 2005). Three plant assemblages have been recognized from the Chahe section, which can be regionally correlated in South China (Nanjing Inst., 1980). The first two assemblages are both composed of filicopsids, pteridosperms, lycopsids and sphenopsids, although the floral diversity decreases afterwards. The third assemblage marks the extinction of the Cathaysian flora. No identifiable plant remains at this stage have been discovered in the Chahe section. Regionally, plant fossils of this stage are also sparse and rare in South China.

The composition of spores and pollen in the Chahe section suggests three distinct evolutionary stages across the

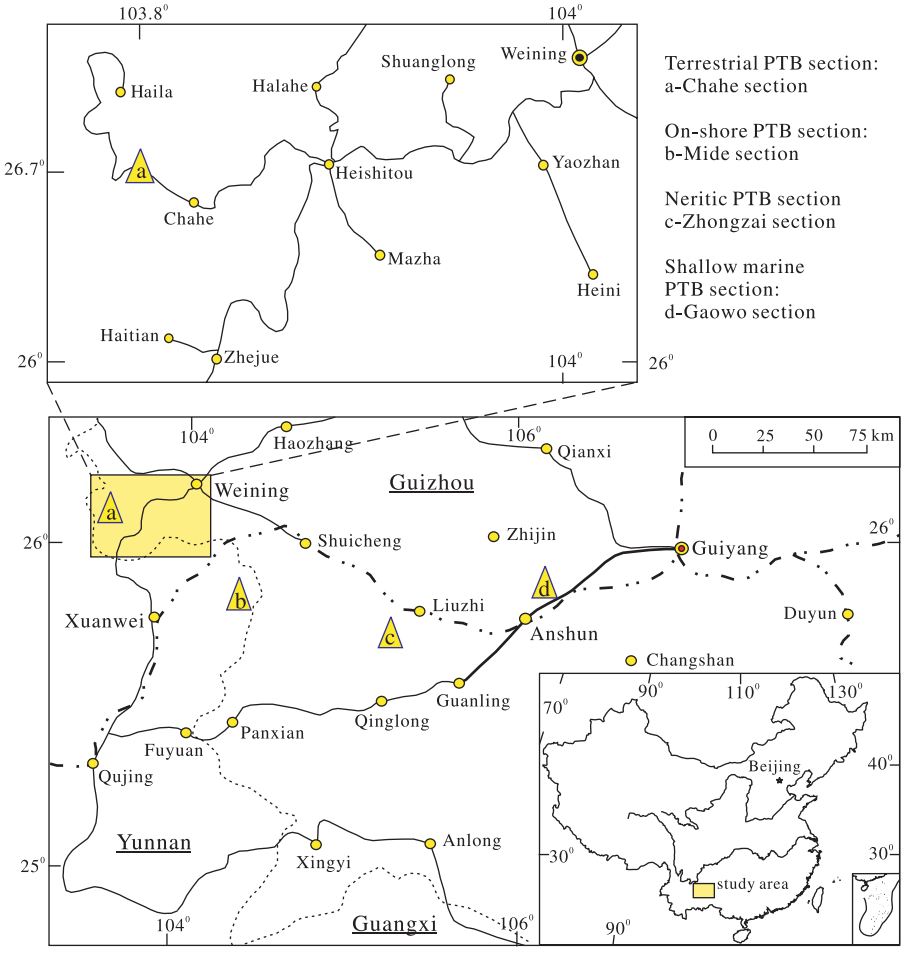

Fig. 1. Geographic map of the study area and position of the Chahe section.

boundary, which accords well with the appearance of macroplant fossils in the same section (Peng et al., 2005). The first Stage (upper part of the Xuanwei Formation) is characterized by Late Permian or Palaeozoic-type ferns and pteridosperms, with a few gymnosperms. Most of them are Paleozoic types with the appearance of some typical Late Permian pollen such as *Lueckisporites*. The second stage (in the PTB clayrocks of the uppermost Xuanwei Formation) is marked by an abrupt drop of sporopollen contents and the mixed flora characteristic of the Late Permian (same as the first stage) and the Early Triassic such as *Lundbladispora* and *Taeniaesporites*, as well as the abundant appearance of fungi spores regionally (Peng et al., 2005). Palynomorphs were still rare in the third stage (the Kayitou Formation) which, coupled with the high content of some typical Early Triassic taxa such as *Lundbladispora*, *Aratrisporites* and *Taeniaesporites*, is dominated by gymnosperm pollen, with limited ferns and pteridosperms.

The PTB of the Chahe section is demarcated and located in the less than 1 m thick PTBST (Peng et al., 2005), which is probably the highest resolution demarcation of the TPTB in the non-marine realm. Across the PTBST, fossils of both plants and palynomorphs change dramatically as what we have outlined above. The $\delta^{13}C_{org}$ across the PTBST at the Chahe section also have the same changing trends similar to those widely found in the marine realm (Peng et al., 2005). Three stages are recognizable at the Chahe section. The stage 1 marks the first big drop of the $\delta^{13}C$ at the start of the PTBST, being coincidence to the dramatic decrease of plants, the stage 2 reflects the recovery trend of the $\delta^{13}C$ in the PTBST, and the stage 3 is another fall of the $\delta^{13}C$ and remains lower values just following the PTBST. The coincidence of $\delta^{13}C$ changing trends across the PTB from marine facies to land might suggest a synchronous collapse of marine and terrestrial ecosystems during the end-Permian biotic crisis (Twitchett et al., 2001).

3. Materials and methods

All samples were obtained from the outcrop sections and were collected as fresh as possible. Nine claystone and/or mudstone samples were analyzed (sample collecting position please refer to Fig. 2). Samples were numbered as GWC-21, GWC-22, GWC-28, GWC-30, GWC-63,

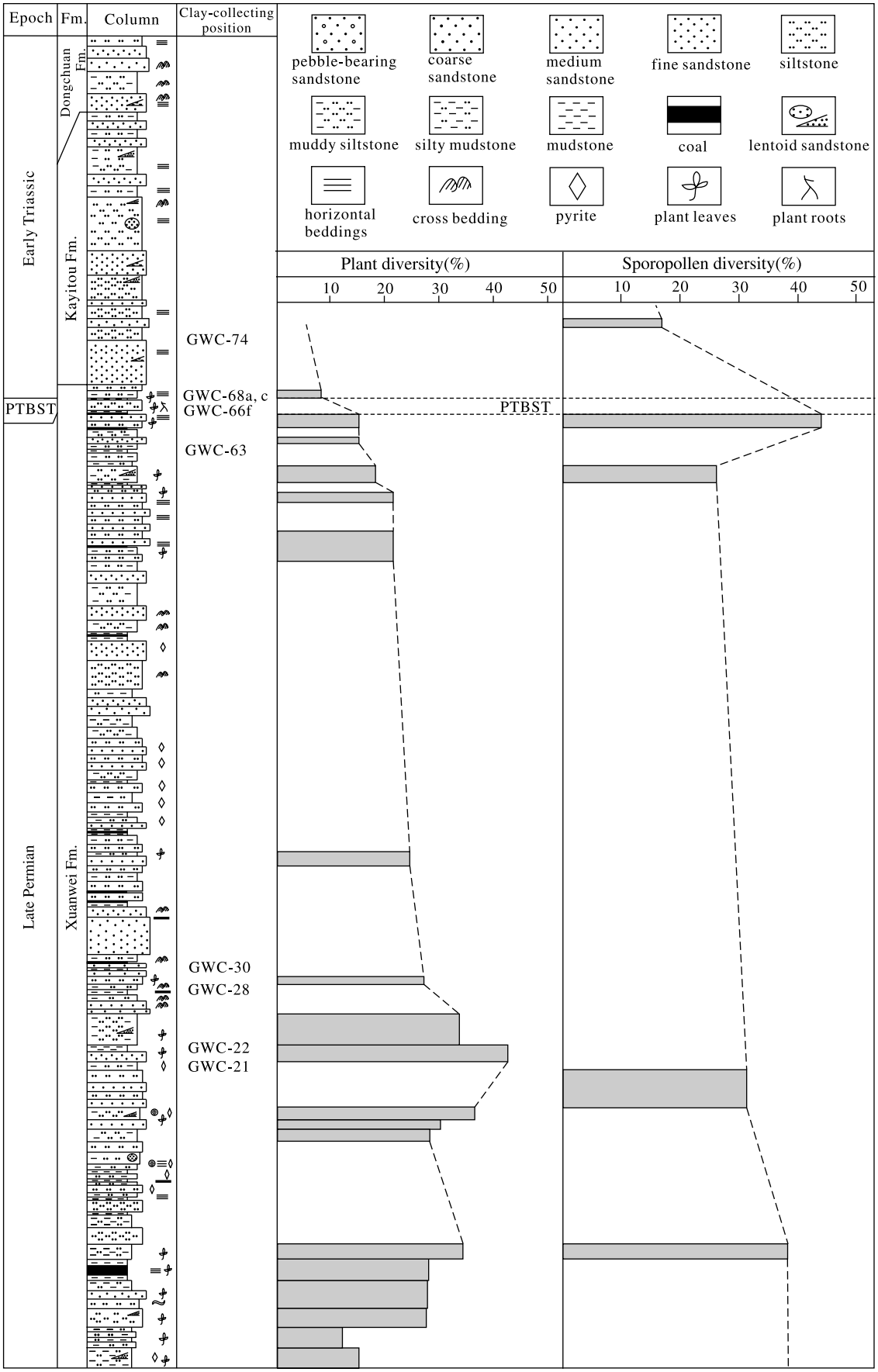

Fig. 2. Stratigraphic column of the Chahe section and clay sampling positions.

GWC-66f, GWC-68a, GWC-68c and GWC-74, respectively. Among them, the samples numbered GWC-68a and GWC-68c are claystones collected from different positions of the same Bed 68. They are treated as repeat samples for verification. Sample GWC-74 is mudstone and all other samples are claystones.

Conventional clay-analyzing techniques were used to treat those samples. First, the samples were treated in order to separate the clays and the debris. All samples were first placed in serial numbered glassy beakers, respectively and marinated by pure water for a couple of days. The muddy samples were then separated into fine colloid clay minerals and coarse clastic grains by panning and then dried. Second, minerals of interest to this study (such as zircons, quartz, etc.) in the clastic fraction were examined and picked out under a binocular microscope. Finally, the separated clays and selected clastic minerals were analyzed by X-ray diffraction (XRD), scanning electronic microscopy (SEM) and X-ray fluorescence spectroscopy (XFS) methods. Clay minerals were analyzed qualitatively and quantitatively by XRD and visually studied by SEM. The selected clastic minerals were observed and identified by SEM. The claystone samples were also analyzed for oxides by XFS.

The XRD used is type D/max-3B and the SEM used is type JSM-35CF. Both were made in Japan. The XFS used is type SRS-303 and was made in Germany. All these instruments are located in the Testing Center of China Universtiy of Geosciences, Wuhan, Hubei Province, P.R. China. GBW standard were applied for testing of oxides, which gives a precision of relative error (RE) less than $\pm$ 0.7% and an accuracy of ΔlgC (difference of standard logarithm of oxides minus testing logarithm of oxides) less than $\pm$0.02.

4. Results

The separated clay minerals and clastic minerals in the claystones and/or mudstones were systematically analyzed. Results are outlined below.

4.1. Clay minerals in the claystones and/or mudstones

The XRD analysis of claystones and/or mudstones in the Chahe section indicates that there are different clay mineral compositions between claystones and/or mudstones in the PTB interval and in the underlying and overlying strata of the PTB interval (Table 1). The clay minerals in the claystones of the PTB interval (nos. GWC-66f, GWC-68a and GWC-68c) are mainly composed of illite–montmorillonite interlayers (70–85%), with a few montmorillonites (10–25%) and chlorites (5%) (Fig. 3, F, G and H). The interlayer percentage of mixed illite–montmorillonite is 75%, which means illite shares 75% and montmorillonite shares 25% of the interlayer composition. However, the other claystones and/or mudstones underlying and overlying the PTB interval are made up of chlorites and/or kaolinites. In the underlying strata, four claystones (nos. GWC-21, GWC-22, GWC-28 and GWC-30) are made up of kaolinite (55–80%) and chlorite (20–45%) (Fig. 3, A, B, C and D) while one (no. GWC-63) consists only of chlorite (100%) (Fig. 3, E). In the overlying strata, the mudstone of Bed 74 (no. GWC-74) also only consists of chlorite of 100% (Fig. 3, I). The composition of illite–montmorillonite interlayers is also characteristic of marine PTB claystones in South China (Yang et al., 1993; Zhang et al., 2002).

The purified clay minerals were studied by SEM as well. The claystones collected from Beds 21, 22, 28 and 30 are mainly composed of irregular sheet kaolinites and tree-leaf shaped chlorites (Fig. 4, A, B, C and D). The claystones and/or mudstone of Beds 63 and 74 are mainly composed of tree-leave shaped chlorites, which were highly crystallized with clear boundaries and obvious tree leaves of crystals (Fig. 4, E and I). However, the claystones of Beds 66 (no. GWC-66f) and 68 (nos. GWC-68a and GWC-68c) are mainly composed of irregular sheet illite–montmorillonite interlayers and a few montmorillonites (Fig. 4, F, G and H). The mixed illite–montmorillonite interlayers of Bed 68 were not well crystallized (Fig. 4, G and H) with unclear crystal boundaries. This can also be recognized from the X-ray

Table 1
Clay mineral compositions and contents in different claystones and/or mudstones of the Chahe section (XRD results)

Time	Bed no.	Coll. no.	Clay mineral composition
Overlying strata	74	GWC-74	Chlorites (100%)
PTB interval	68	GWC-68c[a]	Illite–montmorillonite interlayers (85%)+ Montmorillonites (10%)+ chlorites (5%)
		GWC-68a	Illite–montmorillonite interlayers (70%)+ Montmorillonites (25%)+ chlorites (5%)
	66	GWC-66f	Illite–montmorillonite interlayers (70%)+ Montmorillonites (25%)+ chlorites (5%)
Underlying strata	63	GWC-63	Chlorites (100%)
	30	GWC-30	Kaolinites (80%)+ Chlorites (20%)
	28	GWC-28	Kaolinites (60%)+ Chlorites (40%)
	22	GWC-22	Kaolinites (55%)+ Chlorites (45%)
	21	GWC-21	Kaolinites (55%)+ Chlorites (45%)

[a] GWC-68a and GWC-68c are clay samples collected from different positions of Bed 68, which can be considered as repeated samples for verification.

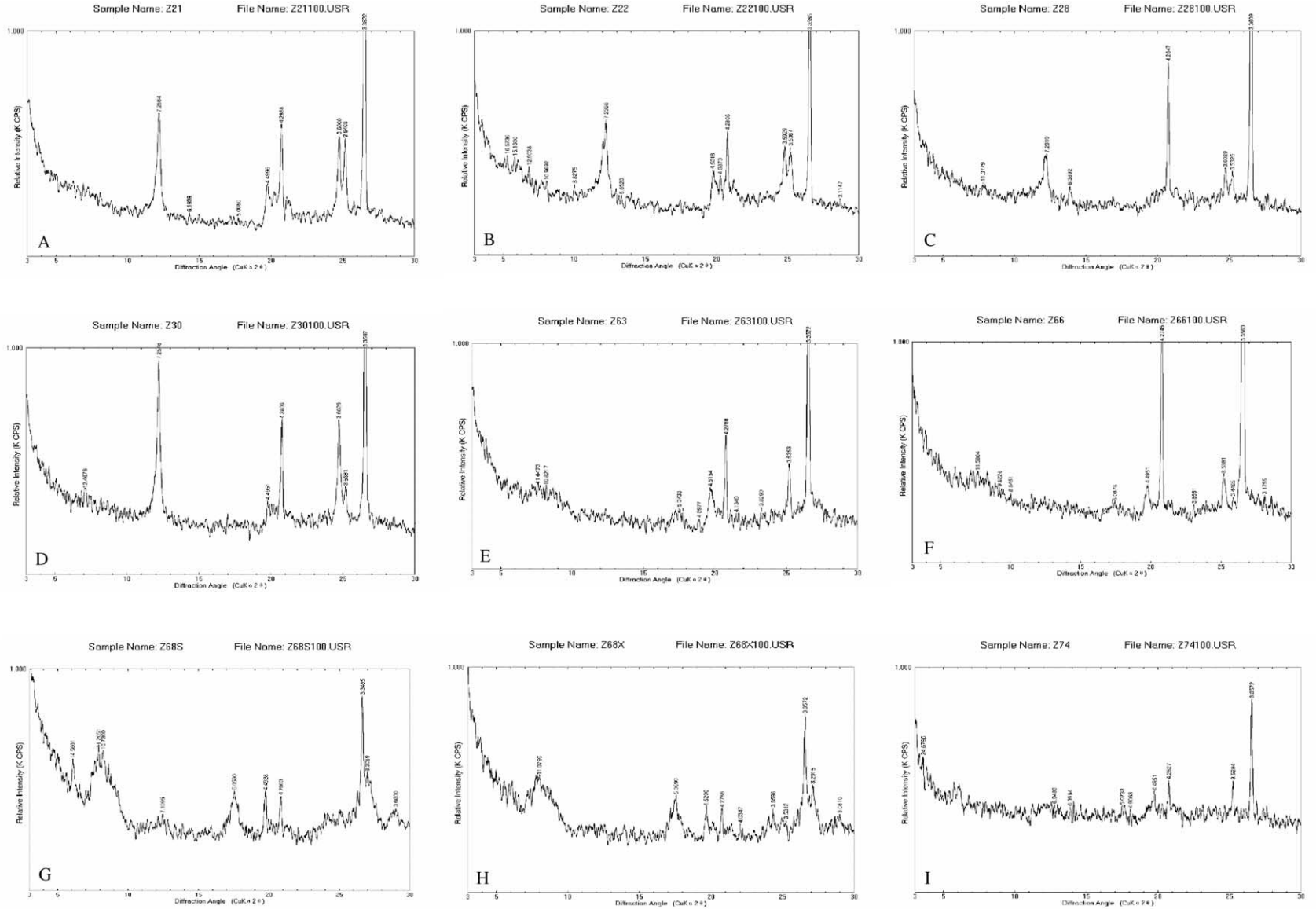

Fig. 3. Graphs X-ray fluorescence spectroscopy (XFS) for the studied samples.

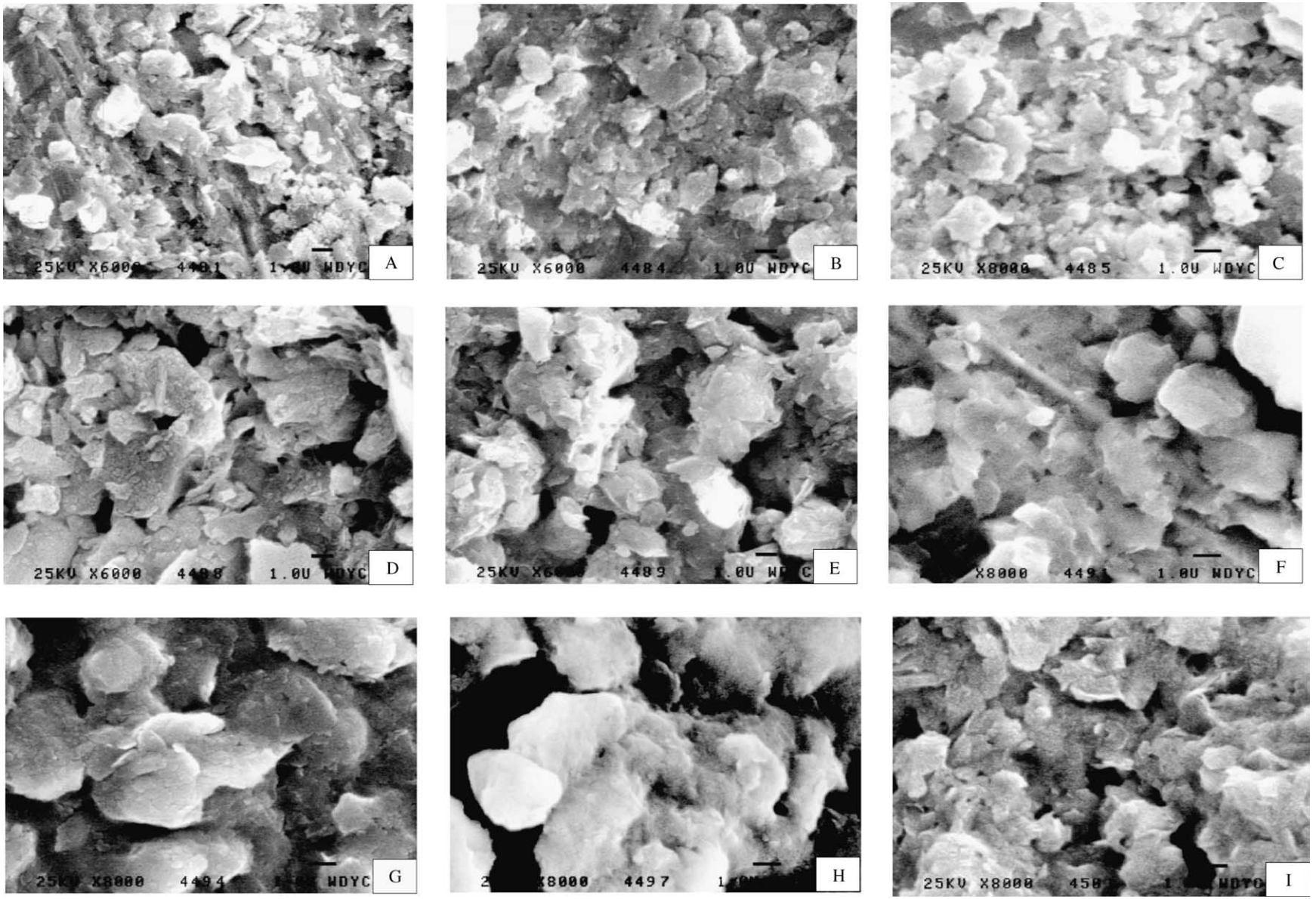

Fig. 4. Clay minerals of studied samples under the scanning electronic microscope (SEM).

diffraction map, which shows a wide and asymmetric diffraction peak for the illite–montmorillonite interlayers (Fig. 3, G and H). The results of XRD agree with those seen from SEM.

4.2. Clastic minerals in the claystones

The remaining clastics in the claystones and/or mudstones after purification and extraction are mainly composed of siliceous, calcareous and ferruginous particles. However, there are some special authigenic clastic minerals (such as hexagonal dipyramid quartz and zircons) in the claystones across the PTB interval (Table 2). They can be classified into two types according to the composition of these claystones and/or mudstones. One type, including sample nos. GWC-21, 22, 28, 30, 63, 68c and 74, is only composed of siliceous, calcareous and ferruginous particles. The other, including sample nos. GWC-66f and 68a, has some special authigenic clastic minerals such as hexagonal dipyramid quartz and zircons (Figs. 5 and 6) as well as siliceous, calcareous and ferruginous particles.

Clastics in the claystones of Beds 21, 22, 28 and 30 are mainly composed of dark-red ferruginous and brownish-yellow argillaceous, irregular particles with a few siliceous and calcareous irregular particles but no well-crystallized hexagonal dipyramid quartz and zircons. Clastics in the claystone of Bed 63 are mainly composed of ivory calcareous and brownish-yellow argillaceous, irregular particles with a few colorless or white siliceous and dark-red ferruginous irregular particles but no well-crystallized hexagonal dipyramid quartz and zircons. Clastics in the mudstone of Bed 74 are mainly composed of dark-red ferruginous and brownish-yellow argillaceous, irregular particles with a few colorless siliceous and white calcareous irregular particles but no well-crystallized hexagonal dipyramid quartz and zircons.

Clastics in the claystone of Bed 66 (sample no GWC-66f) are mainly composed of black ferruginous and brownish-yellow argillaceous, irregular particles with a few colorless or white siliceous and calcareous irregular particles. Clastics in the claystones of Bed 68 (sample nos. GWC-68a and 68c) are mainly composed of ivory and white calcareous and colorless siliceous, irregular particles with a few dark-red ferruginous and brownish-yellow argillaceous irregular particles. Some special authigenic clastic minerals such as hexagonal dipyramid quartz and zircons (Figs. 5 and 6) are only found in the claystones of Bed 66 (sample no. GWC-66f) and Bed 68 (sample no. GWC-68a), although no hexagonal dipyramid quartz and zircons have been found in the repeat sample of Bed 68 (sample no. GWC-68c). Through observation with SEM, we recognize that the hexagonal dipyramid quartz found in Beds 66 and 68 are well crystallized, while slightly rounded and uneven on the crystal surface (Figs. 5 and 6), which indicate they were transported some distance after their formation. This corresponds well to the fluvial sedimentary environment of these beds containing the claystones and/or mudstones (Zhao Quanmin, 2003, PhD thesis of China University of Geosciences). The hexagonal dipyramid quartz found in the claystone of Bed 66 has prismatic faces (Fig. 5), which has not been detected in the hexagonal dipyramid quartz found in the marine PTB sections in South China (Yang et al., 1993), indicating that the terrestrial ones had a relatively longer time for crystallization than the marine ones. The zircons are a combination of tetragonal prisms and tetragonal dipyramids (Figs. 5 and 6). However, no spherules have been found in the claystones across the PTB interval at the Chahe section, which contradicts some previous reports from this area (Wang and Yin, 2001a,b).

The presence of special authigenic clastic minerals, such as hexagonal dipyramid quartz and zircons, is also characteristic of marine PTB claystones (Yang et al., 1993). Although these minerals might also be found in the claystones other than the PTB ones in the marine PTB sections in South China, it is still useful for the correlation

Table 2
Composition of detrital minerals in different claystones and/or mudstones of the Chahe section (SEM results)

Time	Bed no.	Coll. no.	Clastic minerals (particles)
Overlying strata	74	GWC-74	Dark red irregular ferruginous and earth-colored argillaceous + few siliceous and calcareous
PTB interval	68	GWC-68c[a]	Ivory irregular calcareous and siliceous + few ferruginous and argillaceous
		GWC-68a	Ivory irregular calcareous and siliceous + few ferruginous and argillaceous + Hexagonal dipyramid quartz and zircons
	66	GWC-66f	Black irregular ferruginous and earth-colored argillaceous + few siliceous and calcareous + Hexagonal dipyramid quartz and zircons
Underlying strata	63	GWC-63	Ivory irregular calcareous and earth-colored argillaceous + few siliceous and ferruginous
	30	GWC-30	Dark red irregular ferruginous and earth-colored argillaceous + few siliceous and calcareous
	28	GWC-28	Dark red irregular ferruginous and earth-colored argillaceous + few siliceous and calcareous
	22	GWC-22	Dark red irregular ferruginous and earth-colored argillaceous + few siliceous and calcareous
	21	GWC-21	Dark red irregular ferruginous and earth-colored argillaceous + few siliceous and calcareous

[a] GWC-68a and GWC-68c are clay samples collected from different positions of Bed 68, which can be considered as repeated samples for verification.

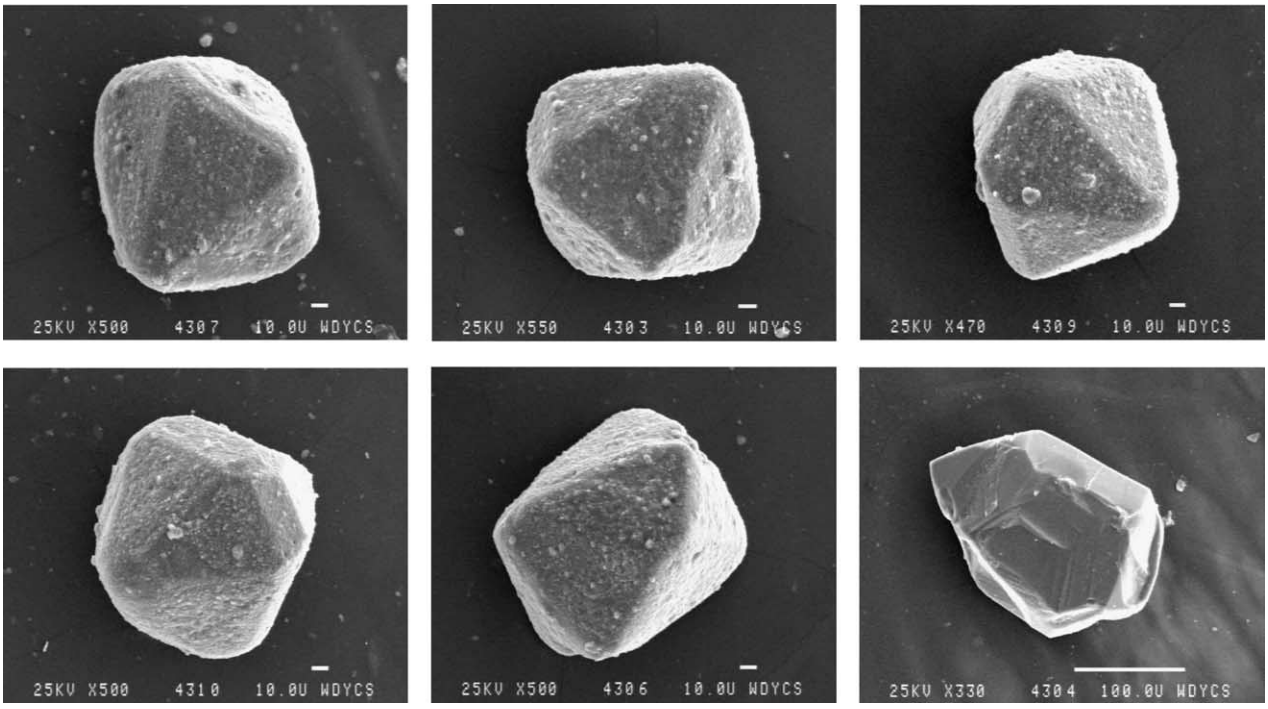

Fig. 5. Clastic minerals of hexagonal dipyramid quartz and zircons in Bed 66f of the Chahe section.

of the PTB from marine facies to land, because the marine PTB claystones are usually easily distinguished by marine fossils. In the TPTB sections, except for these outlined by plant, spore and pollen fossils, the TPTB claystones have unique compositions of clay and clastic minerals, which make them easier to recognize for subdivision and correlation.

4.3. Geochemical composition of the claystones

Oxide contents of the claystones and/or mudstone show peculiar changes across the PTB interval (Table 3, Fig. 7). Among the claystones and/or mudstones, Bed 66 (sample no. GWC-66f) records the highest content of SiO_2 (69.05%) and the lowest content of Al_2O_3 (15.27%). Bed 68 (sample

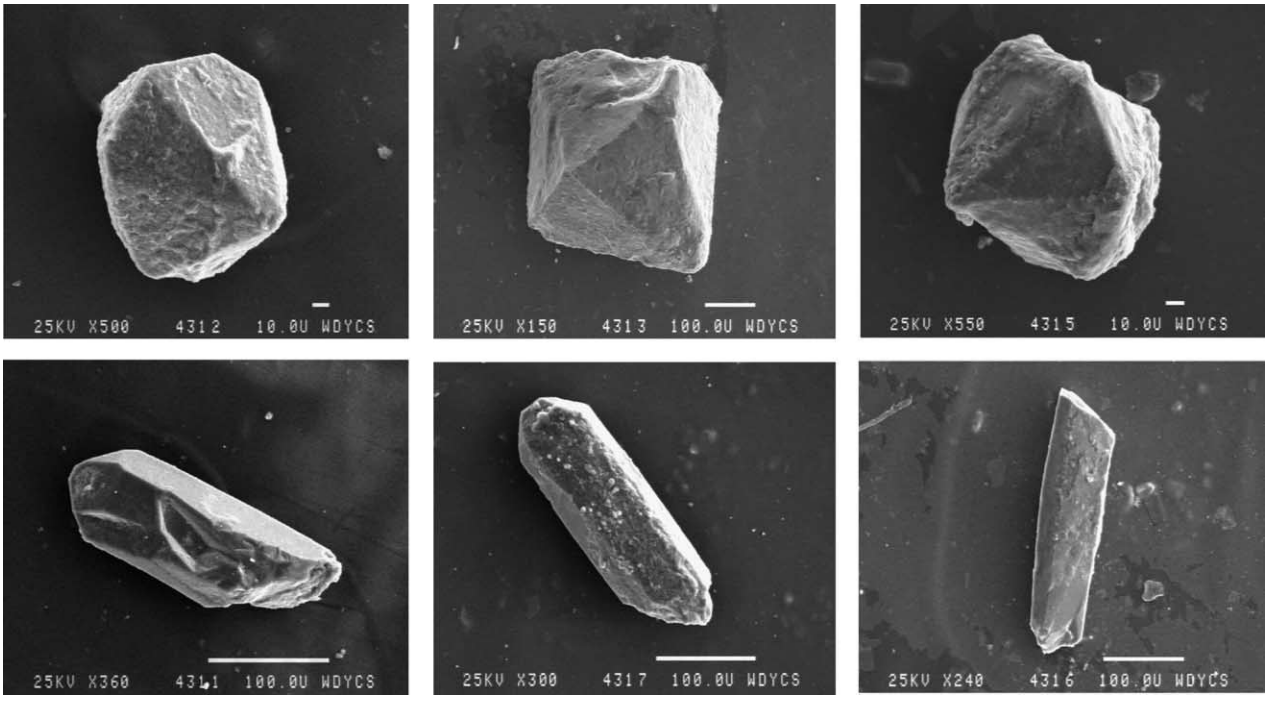

Fig. 6. Clastic minerals of hexagonal dipyramid quartz and zircons in Bed 68a of the Chahe section.

Table 3
Concentrations of oxides in different claystones and/or mudstones of the Chahe section (XFS results)

Oxide	Coll. no.								
	GWC-21	GWC-22	GWC-28	GWC-30	GWC-63	GWC-66f	GWC-68a	GWC-68c[a]	GWC-74
SiO_2	54.72	52.39	60.46	68.29	54.41	69.05	58.43	58.18	45.72
TiO_2	9.22	6.29	5.11	2.18	5.57	2.54	0.72	0.74	5.43
Al_2O_3	30.60	30.70	23.4	20.75	28.22	15.27	24.96	26.89	21.03
TFe_2O_3	1.87	7.65	8.98	5.71	4.44	8.50	6.94	5.54	20.70
MnO	0.01	0.02	0.01	0.36	0.02	0.03	0.39	0.12	0.07
MgO	0.89	1.06	0.56	0.61	1.15	0.78	1.07	0.98	1.99
CaO	0.48	0.54	0.13	0.30	0.53	0.42	0.39	0.36	0.43
K_2O	1.63	1.01	0.98	1.47	5.29	3.29	6.96	7.13	4.19
Na_2O	0.31	0.14	0.19	0.15	0.06	0.075	0.084	0.093	0.075
P_2O_5	0.06	0.13	0.05	0.17	0.11	0.06	0.12	0.07	0.29
Sum of oxides	99.81	99.93	99.87	99.99	99.80	100.02	100.06	100.10	99.93

[a] GWC-68a and GWC-68c are clay samples collected from different positions of Bed 68, which can be considered as repeat samples for verification.

nos. GWC-68a and GWC-68c) records the highest content of K_2O (6.96% and 7.13%) and MnO (0.39% and 0.12%), and the lowest content of TiO_2 (0.72% and 0.74%), respectively. Some trace element concentrations resemble the same kind of changes in claystones across the PTB interval (Zhao Quanmin, 2003, PhD thesis of China University of Geosciences). Cr is highest in Bed 66 and lowest in Bed 68, Zr is lowest in Bed 66, and Co is lowest in Bed 68. The abnormal concentrations of oxides and trace elements were also detected across the marine PTB claystones in South China (Yang et al., 1993).

5. Discussion

The claystones and/or mudstones in the PTB interval and those from above and below this interval have different mineral compositions in the Chahe section. This indicates that claystones in the PTB interval formed through a different process than those outside this interval. The claystones of Beds 21, 22, 28 and 30 consist of kaolinites (55–80%) and chlorites (20–45%), but no clastic minerals of special formation (such as zircons and quartz, etc.). They might have formed in acidic sedimentary environments, because kaolinites are easily formed in an acidic medium. The claystone of Bed 63 and the mudstone of Bed 74 are only composed of chlorite (100%), but no clastic minerals of special formation (such as zircons and quartz, etc.). They might have formed in alkaline sedimentary environments, because chlorites are easily formed in alkaline conditions.

The claystones in Beds 66 and 68 originated from volcanic processes. The claystones in these two beds are mainly composed of illite–montmorillonite interlayers. There are also some special clastic minerals such as hexagonal dipyramid quartz and zircons only found in claystones of these two beds, indicating their unique formation. Hexagonal

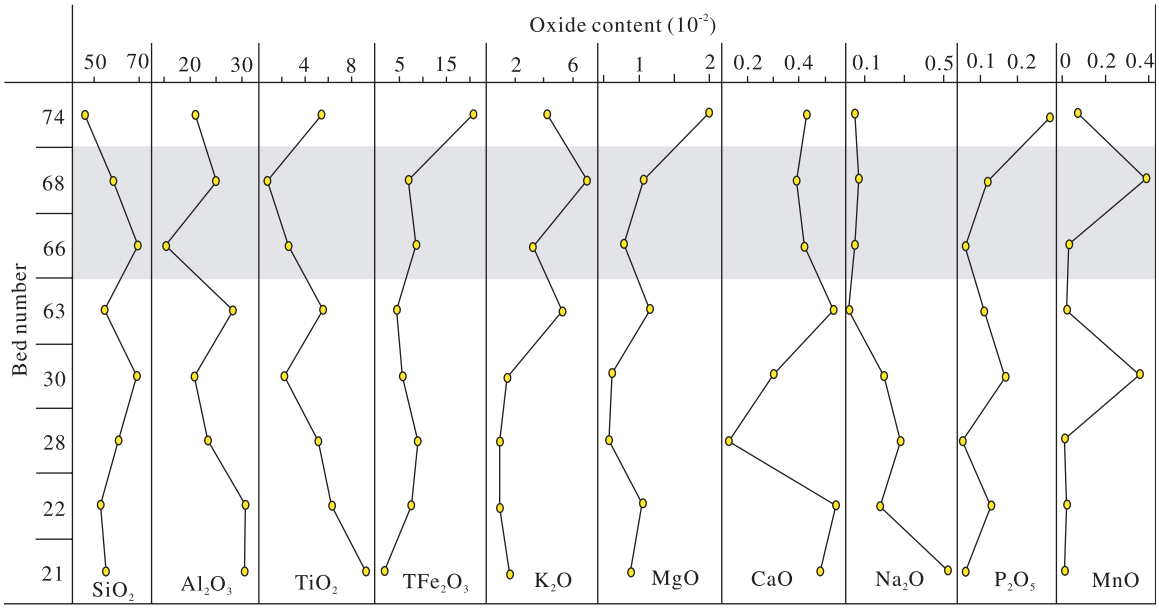

Fig. 7. Variations of oxide concentrations in claystones and/or mudstones of the Chahe section.

dipyramid β-quartz can only form at temperatures between 573 and 867 °C and will only be preserved if rapidly cooled, as high-temperature β-quartz is replaced by low-temperature α-quartz if cooling is slow. So hexagonal dipyramid β-quartz is indicative of rapid cooling of volcanic rocks. In addition, zircons are usually formed in magmatic rocks. This indicates that the claystones in Beds 66 and 68 probably originated by volcanism. Most important is that we did not find spherules in the PTB claystones at the Chahe section nor in marine PTB sections in western Guizhou and eastern Yunnan (details see below), making the idea of extraterrestrial impact during the PTB unsubstantiated.

The trace elements in Beds 66 and 68 at the Chahe section suggest that the dust was highly acidic and therefore also supporting a volcanic origin. The ratio of TiO_2/Al_2O_3 in the claystones can indicate the source of clays (Clark et al., 1986; Zhang et al., 2002), as the ratios of terrigenous claystones range from 0.035 to 0.050, and is less than 0.020 for acid volcanic ash. The TiO_2/Al_2O_3 ratios of Bed 68 range between 0.0275 and 0.0288, indicating that both terrigenous and acid volcanic ashes contributed to the claystone sediments. Increases in SiO_2 and K_2O content in Bed 66 and Bed 68 are also evidence of acid volcanic eruptions. Thus, we hold that the claystones of Beds 66 and 68 between the PTB interval are products of acid volcanic ash accompanying normal sedimentary clays.

6. Correlation of claystones in different facies in South China

Claystones are widely developed in the Late Permian and Early Triassic marine strata in South China. Here, we give an overall review and correlation of those PTB claystones based on our studies in western Guizhou and eastern Yunnan and references for South China (Yang et al., 1993).

Claystones from three other PTB sections from on-shore marine and terrestrial alternate facies to shallow marine facies in western Guizhou and eastern Yunnan, i.e. the Mide, the Zhongzai and the Gaowo sections (see Fig. 1 for position), have been studied. Characteristics of those claystones are summarized in Table 4. Unlike the unique clay mineral composition of the claystones in the PTBST at the Chahe section, claystones in the Mide, Zhongzai and Gaowo sections are all mainly composed of illite–montmorillonite interlayers, regardless of whether they come from the PTBST or not. However, the special authigenic clastic minerals, such as hexagonal dipyramid quartz and zircons, are only found in the PTBST claystones at those sections, indicating the same volcanic origin of those claystones as that in the PTBST of the Chahe section (Table 4). We must emphasize here that no spherules have yet been found in any claystones at those three sections in western Guizhou and eastern Yunnan.

Yang et al. (1993) reported the results of claystone studies of some marine PTB sections from Liangfengya of the Chongqing City, Huangshi of the Hubei Province and Meishan of the Zhejiang Province in the middle and east part of South China (Table 5). Except for samples HE-41 and HE-42 from the Earliest Triassic Daye Formation of the Huangshi area, Hubei Province are mainly composed of illites, while the others are mainly composed of illite–mortmorillonite interlayers, regardless of whether they were collected from the PTBST claystones or not. Another difference in these claystones compared with those in western Guizhou and eastern Yunnan is that they all contain

Table 4
Characteristics and correlation of PTB claystones from marine facies to land in western Guizhou and eastern Yunnan, South China

Facies	Section[a]	Coll. no.	Clay mineral composition	Autogenic minerals			Distance to volcanoes
				H.D. quartz	Zircon	Feldspar	
Shallow marine	Gaowo	GPG52	Illite–montmorillonite interlayers (85%)+ illites (15%)	No	No	No	Far
		GPG50	Illite–montmorillonite interlayers (65%)+ illites (35%)	No	No	No	Far
		GPG47	Illite–montmorillonite interlayers (60%)+ kaolinites (10%)+ illites (30%)	Abundant	A few	Abundant	Close
		GPG45	Illite–montmorillonite interlayers (90%)+ kaolinites (10%)	Abundant	A few	A few	Close
Neritic	Zhongzai	GLZ14	Illite–montmorillonite interlayers (100%)	A few	No	No	Far
		GLZ12	Illite–montmorillonite interlayers (100%)	A few	No	No	Far
On-shore	Mide	YXM39	Illite–montmorillonite interlayers (70%)+ kaolinites (20%)+ chlorites (10%)	No	No	No	Far
		YXM35	Illite–montmorillonite interlayers (65%)+ kaolinites (25%)+ chlorites (10%)	No	No	No	Far
		YXM34	Illite–montmorillonite interlayers (80%)+ kaolinites (15%)+ chlorites (5%)	No	No	No	Far
		YXM32	Illite–montmorillonite interlayers (45%)+ kaolinites (55%)	A few	No	No	Far
Terrestrial	Chahe	GWC68	Illite–montmorillonite interlayers (70%)+ montmorillonites (25%)+ chlorites (5%)	Many	A few	No	Close
		GWC66f	Illite–montmorillonite interlayers (70%)+ montmorillonites (25%)+ chlorites (5%)	Many	A few	No	Close

[a] Positions of these sections refer to Fig. 1. H.D. quartz (hexagonal dipyramid quartz).

Table 5
Characteristics of PTB claystones at some marine PTB sections in South China (after Yang et al., 1993)

Section	Time	Coll. no.	Clay mineral composition	Autogenic minerals		
				H.D. quartz	Zircon	Apatites
Liangfengya, Chongqing	Lowermost Induan	CL-45	Illite–montmorillonite interlayers (100%)	A few	No	No
	Uppermost Changhsingian	CL-43	Illite–montmorillonite interlayers (100%)	Rare	No	A few
		CL-41	Illite–montmorillonite interlayers (100%)	Rare	No	No
		CL-39	Illite–montmorillonite interlayers (main) + montmorillonites (some)	A few	No	No
Huangshi, Hubei	Lowermost Induan	HE-42	Illites (97.2%)+ kaolinites (2.8%)	–	–	–
		HE-41	Illites (97.7%)+ kaolinites (2.3%)	–	–	–
		HE-38	Illite–montmorillonite interlayers (91.6%)+ kaolinites (8.4%)	Abundant	A few	No
		HE-34	Illite–montmorillonite interlayers (95.4%)+ kaolinites (4.6%)	A few	A few	Many
	Uppermost Changhsingian	HE-31	Illite–montmorillonite interlayers (97.7%)+ kaolinites (2.3%)	No	A few	A few
Meishan, Zhejiang	Lowermost Induan	ZCB-4	Illite–montmorillonite interlayers (91.5%)+ kaolinites (8.5%)	Rare	A few	Rare
		ZCB-3	Illite–montmorillonite interlayers (89.9%)+ kaolinites (10.1%)	Abundant	A few	Rare
	Uppermost Changhsingian	ZCB-2	Illite–montmorillonite interlayers (46.1%)+ kaolinites (7.8%)+ illites (46.1%)	Rare	A few	A few
		ZCB-1	Illite–montmorillonite interlayers (97.1%)+ kaolinites (2.9%)	Abundant	A few	A few

some special authigenic clastic minerals like hexagonal dipyramid quartz or zircons, probably indicating that more volcanic activity occurred in the middle and eastern part of South China than that in the western part of South China, where the study area of western Guizhou and eastern Yunnan locates.

7. Conclusions

As indicated by biostratigraphy, claystones in the TPTB interval of the Chahe section have different clay mineral compositions compared to claystones overlying and underlying the PTB interval. The recognition of some special authigenic clastic minerals such as hexagonal dipyramid quartz and zircons in claystones in the PTB interval show their unique volcanic origin during that time. In addition, no spherules of extraterrestrial impact origin are found in any of those PTB claystones in western Guizhou and eastern Yunnan. The two claystones of volcanic origin at the Chahe section clearly define the event boundary of the TPTB as do the marine PTB claystones, and thus are good markers for high-resolution subdivision and correlation of the PTB from marine facies to land in South China.

Acknowledgments

This work is part of the research programs supported by the National Science Foundation of China (Grant nos. 40172012, 40232025 and 40325004). Peng Yuanqiao acknowledges support of Australian Commonwealth Government and Deakin University for the award of an International Postgraduate Research Scholarship (IPRS). The authors are grateful to Prof. Shuzhong Shen (Nanjing Institute of Geology and Palaeontology, Academia Sinica, P. R. China) and Prof. Valentin Krassilov (University of Haifa, Israel) for their critical and constructive reviews and comments. Dr Monica Campi (Deakin University, Australia) is acknowledged for the revisions and suggestions of the manuscript.

References

Basu, A.R., Petaev, M.I., Poreda, R.J., Jacobsen, S.B., Becker, L., 2003. Chondritic meteorite fragments associated with the Permian–Triassic boundary in Antarctica. Science 302, 1388–1392.

Becker, L., Poreda, R.J., Hunt, A.G., Bunch, T.E., Rampino, M., 2001. Impact event at the Permian–Triassic boundary: evidence from extraterrestrial noble gases in fullerene. Science 291, 1530–1533.

Bowring, S.A., Erwin, D.W., Jin, Y.G., Martin, M.W., Davidek, K., Wang, W., 1998. U/Pb zircon geochronology and tempo of the end-Permian mass extinction. Science 280, 1039–1045.

Braun, T., Osawa, E., Detre, C., Tóth, I., 2001. On some analytical aspects of the determination of fullerenes in samples from the Permian/Triassic boundary layers. Chemical Physics Letters 348, 361–362.

Buseck, P.R., 2002. Geological fullerenes: review and analysis. Earth and Planetary Science Letters 203, 781–792.

Clark, D.L., Wang, C.Y., Orth, C.J., Gilmore, J.S., 1986. Conodont survival and the low iridium abundances across the Permian–Triassic boundary in South China. Science 233, 984–986.

Erwin, D.H., 2003. Impact at the Permo-Triassic boundary: a critical evaluation. Astrobiology 3, 67–74.

Farley, K.A., Mukhopadhyay, S., Isozaki, Y., Becker, L., Poreda, R.J., 2001. An extraterrestrial impact at the Permian–Triassic boundary? Science 293, 2343.

Kaiho, K., Kajiwara, Y., Nakano, T., Miura, Y., Kawahata, H., Tazaki, K., Ueshima, M., Chen, Z.Q., Shi, G.R., 2001. End-Permian catastrophe by a bolide impact: evidence of a gigantic release of sulfur from the mantle. Geology 29, 815–818.

Koeberl, C., Gilmour, I., Reimold, W.U., Claeys, P., Ivanov, B., 2002. End-Permian catastrophe by a bolide impact: evidence of a gigantic release of sulfur from the mantle: comment. Geology 30, 855.

Mundil, R.L., Metcalfe, I., Ludwig, K., Paull, R., Oberli, F., Nicoll, R., 2001. Timing of the Permian–Triassic biotic crisis: implication from new zircon U/Pb age data. Earth and Planetary Science Letters 187, 131–145.

Mundil, R., Ludwig, K.R., Metcalfe, I., Renne, P.R., 2004. Age and timing of the Permian mass extinction: U/Pb dating of closed-system zircons. Science 305, 1760–1763.

Nanjing Institute of Geology and Palaeontology, Academica Sinica, 1980. Late Permian coal-bearing strata and Palaeontological fauna in Western Guizhou and Eastern Yunnan. Science Press, Beijing, 277pp (in Chinese).

Peng, Y.Q., Tong, J.N., Shi, G.R., Hansen, H.J., 2001. The Permian-Triassic boundary set: characteristics and correlation. Newsletters on Stratigraphy 39, 55–71.

Peng, Y.Q., Wang, S.Y., Wang, Y.F., Yang, F.Q., 2002. A proposed area for study of accessory section and point of terrestrial Permian–Triassic boundary. Journal of China University of Geosciences 13, 157–162.

Peng, Y.Q., Zhang, S.X., Yu, J.X., Yang, F.Q., Gao, Y.Q., Shi, G.R., 2005. High-resolution terrestrial Permian–Triassic eventostratigraphic boundary in western Guizhou and eastern Yunnan, southwestern China. Palaeogeography, Palaeoclimatology, Palaeoecology 215, 285–295.

Renne, P.R., Zhang, Z.C., Richard, M.A., Black, M.T., Basu, A.R., 1995. Synchrony and causal relations between Permo-Triassic boundary crisis and Siberian flood volcanism. Science 269, 1413–1416.

Twitchett, R.J., Looy, C.V., Morante, R., Visscher, H., Wignall, P.B., 2001. Rapid and synchronous collapse of marine and terrestrial ecosystems during the end-Permian biotic crisis. Geology 29, 351–354.

Wang, S.Y., 2001. On Kayitou Formation. Journal of Stratigraphy 25, 129–134 (in Chinese with English abstract).

Wang, S.Y., 2002. On Kayitou Formation once again. Journal of Stratigraphy 26, 238–240 (in Chinese with English abstract).

Wang, S.Y., Yin, H.F., 2001a. Study on Terrestrial Permian–Triassic Boundary in Eastern Yunnan and Western Guizhou. China University of Geosciences Press, Wuhan, 87pp (in Chinese with English abstract).

Wang, S.Y., Yin, H.F., 2001b. Discovery of microspherules in claystone near the terrestrial Permian–Triassic boundary. Geological Review 47, 411–414 (in Chinese with English abstract).

Yang, Z.Y., Wu, S.B., Yin, H.F., Xu, G.R., Zhang, K.X., Bi, X.M., 1993. Permo-Triassic Events of South China. Geological Publishing House, Beijing, 153pp.

Yin, H.F., Huang, S.J., Zhang, K.X., Hansen, H.J., Yang, F.Q., Ding, M.H., Bi, X.M., 1992. The effects of volcanism on the Permo-Triassic mass extinction in South China. In: Sweet, W.C., Yang, Z.Y., Dickins, J.M., Yin, H.F. (Eds.), Permo-Triassic Events in the Eastern Tethys. Cambridge University Press, Cambridge, pp. 146–157.

Zhang, S.X., Liu, J.P., Xiao, S.Q., 2002. Study on Permian–Triassic boundary claystones of Duanshan, Guizhou Province. Earth Science-Journal of China University of Geosciences 27, 259–264 (in Chinese with English abstract).

Zhou, Y.Q., Chai, Z.F., Ma, X.Y., Ma, S.L., Ma, J.G., Kong, P., He, J.W., 1991. A mixing model—the elemental geochemistry of Permian–Triassic boundaries in South China and its implication. Geological Review 37, 51–63 (in Chinese).